Research Article | Vol. 30, No. 17 / 15 Aug 2022 / Optics Express 30666
Optics EXPRESS

Graphene-based fine tuning of Fano resonance transmission of quasi-bound states in the continuum

MYUNGHWAN KIM,[1] CHUL-SIK KEE,[2,3] AND SOEUN KIM[1,4]

[1]Division of Applied Photonics System Research, Advanced Photonics Research Institute, Gwangju Institute of Science and Technology, Gwangju 61005, Republic of Korea
[2]Division of Frontier Photonics Research, Advanced Photonics Research Institute, Gwangju Institute of Science and Technology, Gwangju 61005, Republic of Korea
[3]cskee@gist.ac.kr
[4]sekim@gist.ac.kr

Abstract: Quasi-bound state in the continuum (BIC) has significant potential because it supports an ultra-high quality factor (Q-factor). Here, we propose a graphene-embedded subwavelength grating that supports quasi-BIC for tuning very sharp Fano resonance transmission. The strongly enhanced light-graphene interaction from the quasi-BIC enables fine variation of the transmission at the resonant wavelength. The Q-factor of quasi-BIC significantly decreases as the Fermi level of graphene increases. We also propose a low-energy consumption THz-wave modulator using this scheme. The designed modulator shows approximately 100% modulation depth with a Fermi level shift of only $E_F = 90$ meV.

1. Introduction

Bound states in the continuum (BICs) are special localized states in the continuum of the radiation spectrum. They originate from geometrical symmetry or destructive interference between radiating waves [1–3]. Therefore, a BIC is characterized as a non-radiating cavity mode. Since the BIC mode supports an infinite quality factor (Q-factor), this mode cannot be coupled with radiating waves. In contrast, the quasi-BIC mode is a resonant mode with a finite Q-factor and can be excited by incident light close to the BIC wavelength by breaking the BIC condition [4].

Since the quasi-BIC mode induces Fano resonance with an ultra-high Q-factor, it has been utilized in various applications, as the high Q-factor enhances light-matter interaction [5–9]. In addition, the quasi-BIC mode can be realized in subwavelength gratings and one-dimensional (1D) photonic crystal (PC) structures, and a high Q-factor is maintained even in the imperfect structures due to fabrication errors, such as tiled, imperfectly etched, or bent structures [10–14]. Although many studies have been conducted on the BIC and quasi-BIC, there is a lack of the research on tuning of Fano resonance by quasi-BIC in the terahertz (THz) band (0.1 ~ 10THz), which has unique potential applications in various fields, such as security imaging, spectroscopy, radar, and wireless high-speed communications [15–17].

Here, we investigate the tuning of Fano resonance using graphene's tunable property in the THz range. In recent years, graphene has emerged as a promising active material for tuning the resonance owing to its outstanding property of gate-tunable carrier concentration [18,19], but its tuning range is very low due to the low light-graphene interaction. In the proposed scheme, the high Q-factor of the quasi-BIC mode enhances the light-graphene interaction, and the transmission at the resonant wavelength changes sharply with a small Fermi level shift.

We also propose a low-energy consumption graphene-based THz-wave modulator using the quasi-BIC mode. Although THz modulators play a key role in THz communications, achieving high-performance THz-wave modulators is challenging because finding an active material in

#468890 https://doi.org/10.1364/OE.468890
Journal © 2022 Received 26 Jun 2022; revised 27 Jul 2022; accepted 27 Jul 2022; published 5 Aug 2022

Optics EXPRESS

the THz band is difficult [20,21]. To solve this problem, graphene-based modulators using plasmonic resonances have been proposed such as inserting graphene into metamaterials, graphene metasurfaces, and graphene antennas using graphene plasmons [22–26]. The resonances enhance the light-graphene interaction, and high-performance modulation has been achieved.

However, the proposed structures are complicated and require a high Fermi level ($E_F > 0.4$ eV) for a high modulation depth, which results in high-energy consumption and the breakdown voltage issue [27]. In addition, since the Q-factor of graphene plasmon resonance decreases with a decrease in mobility, high-quality graphene is required for a high modulation depth [28]. However, in the proposed scheme, we achieve a modulation depth of approximately 100% with a very small Fermi level shift of only 50 meV. Quasi-BIC with a high Q-factor enhances the light-graphene interaction and amplifies the tunable effect of graphene through the Fermi level shift. All simulations were carried out using the finite-element-method (COMSOL Multiphysics software).

2. Tuning of Fano resonance

Figure 1 shows a schematic of the proposed subwavelength grating for quasi-BIC. It consists of a 1D high-resistivity silicon-based grating, upon which double-layer graphene (DLG) with a 5 nm gap (g) is placed. DLG is used for the electrical doping of graphene, and it is implemented by applying a gate voltage between the two graphene layers. We assumed SiO_2 as the background material for the convenience of simulation. The refractive indices of Si and SiO_2 are $n_{Si} = 3.4$ and $n_{SiO2} = 1.98$, respectively [29,30]. The conductivity of graphene can be calculated by the Kubo formula [31–33] as follows:

$$\sigma = \frac{2e^2}{\pi\hbar}\frac{i}{\omega+i/\tau}\ln\left[2\cosh\left(\frac{E_F}{2k_BT}\right)\right] + \frac{e^2}{4\hbar}\left[H(\omega/2) + \frac{4i\omega}{\pi}\int_0^\infty \frac{H(x)-H(\omega/2)}{\omega^2-4x^2}dx\right] \quad (1)$$

$$H(x) = \frac{\sinh(\hbar x/k_BT)}{\cosh(E_F/k_BT)+\cosh(\hbar x/k_BT)}$$

where e is the electron's charge, k_B is Boltzmann's constant, T is the temperature, ω is the angular frequency, $\hbar$ is Planck's constant. From the conductivity of graphene, the permittivity of graphene can be obtained by

$$\varepsilon_G = 1 + \frac{i\sigma}{\omega\varepsilon_0 d_G} \quad (2)$$

where ε_0 is the vacuum permittivity, and d_G is the thickness of graphene ($d_G = 0.34$ nm).

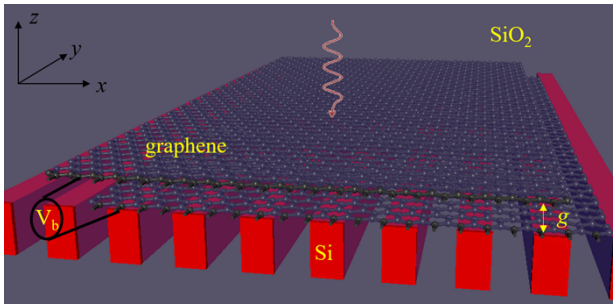

Fig. 1. Schematic diagram of a 1D Si grating with DGL. DLG is placed on the Si grating. The background material is SiO_2.

Figure 2 shows the transmission spectrum of the 1D Si grating structure (without DLG) as a function of the incident angle for transverse magnetic (TM) polarization. The relation of wavelength and incident angle can be easily transformed to the dispersion relation of frequency

Optics EXPRESS

and wave vector of the 1D Si grating. The following parameters are used: period, $a = 137$ μm, height of Si, $h = 0.5a$, and fill factor, $f = 0.3$. In subwavelength grating structures, BICs appear when the radiation channel vanishes due to the simultaneous destructive interference of all radiating waves in the direction of the radiation channel. In the designed structure, the BIC phenomenon occurs accidentally near λ of ~ 355 μm and θ of ~ 14°, and the transmission resonance disappears in this region due to the infinite Q-factor.

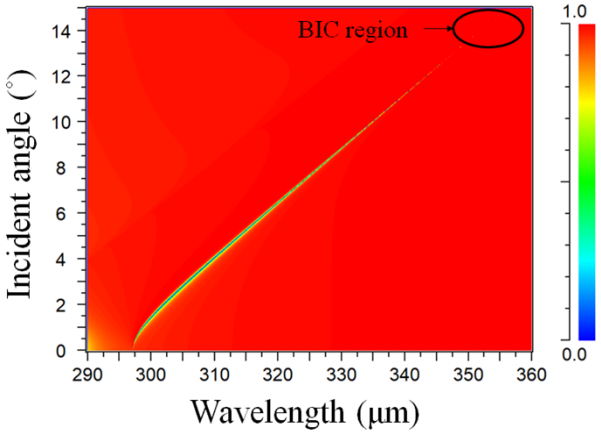

Fig. 2. Transmission spectrum as a function of the incident angle. The period is a = 137 μm, the height of the grating is $h = 0.5a$, and the fill factor is f = 0.3.

Figure 3(a) shows the transmission spectra of the designed grating with DLG for the Fermi level variation from $E_F = 0$ to 50 meV. The same parameters employed in the previous calculation are used, and the incident angle is assumed to be $\theta = 12.5°$, which is chosen for the quasi-BIC mode to support a high Q-factor. The resonant transmission is attributed to the interference between the incident wave and quasi-BIC, that is, Fano resonance transmission. Since the chosen incident angle for the quasi-BIC is very close to the incident angle for the BIC with the infinite Q-factor, the very sharp Fano resonance transmission is observed when $E_F = 0$ eV. As the Fermi level increases, the transmission at the resonant wavelength, T_{dip}, significantly increases. The ultra-high Q-factor enhances the light-graphene interaction, resulting in very high transmission variation. The Q-factor is inversely proportional to the material loss. When E_F increases, the

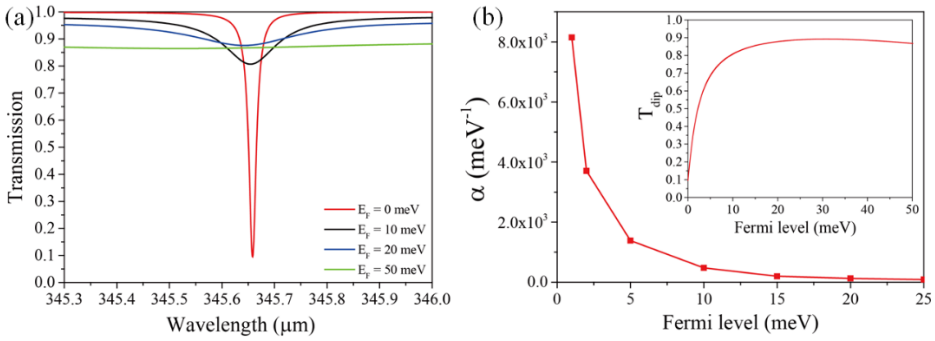

Fig. 3. Transmission spectra for Fermi level variation from E_F = 0 meV to 50 meV. The incident angle is θ = 12.5° (b) α (the ratio of the variation of Q-factor and the variation of E_F) as a function of E_F. The inset shows T_{dip} as a function of E_F.

Optics EXPRESS

loss of the doped graphene notably increases. Thus, it is easily expected that the values of transmission dip and the full half width maximum (FHWM) increase when E_F increases, that is, the Q-factors decrease when E_F increases. Figure to show the dependence of the Q-factor on E_F was provided in the supplement material (Fig. S1). The Q-factors for $E_F = 0$, 10, 20, and 50 meV are $Q = 2.09\times10^4$, 2.56×10^3, 935, and 0 (no resonance), respectively.

The Q-factor significantly decreases, even though E_F increases very little. It is worthy to investigate in quantity the ratio of the variation of Q-factor and the variation of E_F, $\alpha = \Delta Q/\Delta E_F$. α is about 10^3/meV as shown in Fig. 3(b). This means that the shapes of Fano resonance transmission spectra are extremely sensitive to E_F below 10 meV. The inset of Fig. 3(b) shows the values of T_{dip} as a function of E_F. It increases rapidly from 0.095 to 0.802 for the very small variation of E_F from 0 to 10 meV. For $E_F > 30$ meV, T_{dip} decreases as E_F increases because the loss of graphene is the dominant.

3. THz-wave modulator

Using this tunable property, we designed a THz-wave modulator. Figure 4(a) shows the transmission spectra of the designed modulator for the Fermi level variation from $E_F = 0$ eV to 50 meV. The same parameters employed in the previous calculation are used, and the incident angle is only changed from $\theta = 12.5°$ to 1.4° to achieve zero transmission. As shown in Fig. 4, for $E_F = 0$ eV, the transmission dip occurs at $\lambda = 300$ μm, and T_{dip} is almost zero at this wavelength. The minimum value of T_{dip} is determined by the ratio of the loss and coupling coefficient, and the critical coupling condition for zero transmission is satisfied at the chosen parameters. The Q-factors for $E_F = 0$, 10, 20, and 50 meV are $Q = 968$, 667, 469, and 160, respectively.

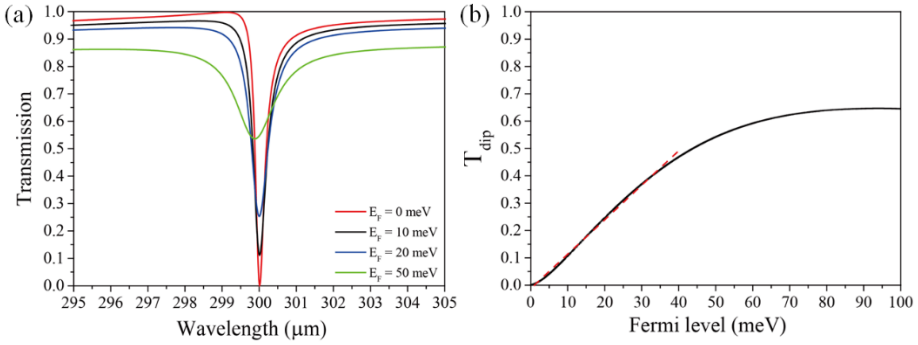

Fig. 4. Transmission spectra for Fermi level variation from E_F = 0 to 50 meV. The incident angle is θ = 1.4°. (b) Tdip (solid black line) as a function of Fermi level from E_F = 0 to 100 meV and the fitted linear relation (dashed red line) of T_{dip} and E_F below 40 meV.

As the Fermi level increases, T_{dip} increases, as mentioned previously. T_{dip} increases almost linearly from 0 to 0.4 when E_F increases from 0 to 35 meV. The fitted linear relation of T_{dip} and E_F is $T_{dip} = 12.65\ E_F$ (eV). This relation is very useful for tuning the transmission to a specific value. We calculated the modulation depth as $MD = (T_{on}\text{-}T_{off})/T_{on}$. When the on-state and off-state are assumed to be $E_F = 90$ and 0 meV, respectively, a modulation depth of ~100% and insertion loss of 36% are achieved. Compared to the previously reported graphene-based modulators, the required Fermi level shift for modulation is approximately fivefold smaller.

The DLG optical modulators have been successfully fabricated by a ridge Si waveguide on a SiO_2 substrate [34,35]. The proposed low-voltage THz transmission modulator can be implemented by an array of ridge Si waveguides on SiO_2 substrate with a DLG. The array of ridge Si waveguides with a period of a length of one hundred microns can be easily fabricated by using conventional lithography techniques [36]. A graphene sheet grown by chemical vapor deposition

Optics EXPRESS

[27,28,34] was then mechanically transferred onto the SiO_2 substrate. Platinum electrodes are deposited on the top and bottom of the graphene layers. Therefore, high efficient modulation performance of the proposed structure can be realized by current fabrication technologies.

4. Conclusion

We proposed a graphene-embedded 1D subwavelength grating that supports quasi-BIC for tuning Fano resonance. The enhanced light-graphene interaction from the quasi-BIC enables a sharp transmission variation with a small Fermi level shift. T_{dip} (Q-factor) varies from 0.095 (2.09×10^4) to 0.892 (935) when E_F does 0 to 20 meV. Using this scheme, we proposed a high-performance graphene-based THz-wave modulator. The high Q-factor of quasi-BIC intensified the graphene loss and matched the critical coupling condition. The designed modulator achieved a very high modulation depth of ~100% and an insertion loss of 36% with a very small Fermi level shift of 90 meV. These promising features will likely generate new avenues for low-energy-consumption graphene-based THz devices.

Funding. National Research Foundation of Korea (2019R1I1A1A01061983, 2020R1F1A1050227, 2022R1I1A1A01072624); Gwangju Institute of Science and Technology (2022).

Disclosures. The authors declare no conflicts of interest.

Data availability. Data underlying the results presented in this paper are not publicly available at this time but may be obtained from the authors upon reasonable request.

Supplemental document. See Supplement 1 for supporting content.

References

1. C. W. Hsu, B. Zhen, A. D. Stone, and J. D. Joannopoulos, "Bound states in the continuum," Nat. Rev. Mater. **1**(9), 16048–13 (2016).
2. S. I. Azzam and A. V. Kildishev, "Photonic Bound States in the Continuum: From Basics to Applications," Adv. Opt. Mater. **9**(1), 2001469 (2021).
3. A. I. Ovcharenko, C. Blanchard, J. P. Hugonin, and C. Sauvan, "Bound states in the continuum in symmetric and asymmetric photonic crystal slabs," Phys. Rev. B **101**(15), 155303 (2020).
4. S. Joseph, S. Pandey, S. Sarkar, and J. Joseph, *Bound States in the Continuum in Resonant Nanostructures: An Overview of Engineered Materials for Tailored Applications* (2021), 10(17).
5. L. L. Doskolovich, E. A. Bezus, and D. A. Bykov, "Integrated flat-top reflection filters operating near bound states in the continuum," Photonics Res. **7**(11), 1314 (2019).
6. A. Kodigala, T. Lepetit, Q. Gu, B. Bahari, Y. Fainman, and B. Kanté, "Lasing action from photonic bound states in continuum," Nature **541**(7636), 196–199 (2017).
7. F. Wu, D. Liu, and S. Xiao, "Bandwidth-tunable near-infrared perfect absorption of graphene in a compound grating waveguide structure supporting quasi-bound states in the continuum," Opt. Express **29**(25), 41975–41989 (2021).
8. X. Wang, J. Duan, W. Chen, C. Zhou, T. Liu, and S. Xiao, "Controlling light absorption of graphene at critical coupling through magnetic dipole quasi-bound states in the continuum resonance," Phys. Rev. B **102**(15), 155432 (2020).
9. Z. Liu, Y. Xu, Y. Lin, J. Xiang, T. Feng, Q. Cao, J. Li, S. Lan, and J. Liu, "High-Q quasibound states in the continuum for nonlinear metasurfaces," Phys. Rev. Lett. **123**(25), 253901 (2019).
10. J. Lee, B. Zhen, S. L. Chua, W. Qiu, J. D. Joannopoulos, M. Soljačić, and O. Shapira, "Observation and differentiation of unique high-Q optical resonances near zero wave vector in macroscopic photonic crystal slabs," Phys. Rev. Lett. **109**(6), 1–5 (2012).
11. H. M. Doeleman, F. Monticone, W. Den Hollander, A. Alù, and A. F. Koenderink, "Experimental observation of a polarization vortex at an optical bound state in the continuum," Nat. Photonics **12**(7), 397–401 (2018).
12. F. Wu, M. Luo, J. Wu, C. Fan, X. Qi, Y. Jian, D. Liu, S. Xiao, G. Chen, H. Jiang, Y. Sun, and H. Chen, "Dual quasibound states in the continuum in compound grating waveguide structures for large positive and negative Goos-Hänchen shifts with perfect reflection," Phys. Rev. A **104**(2), 023518 (2021).
13. C. W. Hsu, B. Zhen, S. L. Chua, S. G. Johnson, J. D. Joannopoulos, and M. Soljačić, "Bloch surface eigenstates within the radiation continuum," Light Sci. Appl. **2**(7), e84 (2013).
14. C. W. Hsu, B. Zhen, J. Lee, S. L. Chua, S. G. Johnson, J. D. Joannopoulos, and M. Soljačić, "Observation of trapped light within the radiation continuum," Nature **499**(7457), 188–191 (2013).
15. A. Y. Pawar, D. D. Sonawane, K. B. Erande, and D. V. Derle, "Terahertz technology and its applications," Drug Invent. Today **5**(2), 157–163 (2013).
16. M. Tonouchi, "Cutting-edge terahertz technology," Nat. Photonics **1**(2), 97–105 (2007).

Optics EXPRESS

17. H. J. Song and T. Nagatsuma, "Present and future of terahertz communications," IEEE Trans. Terahertz Sci. Technol. **1**(1), 256–263 (2011).
18. K. S. Novoselov, A. K. Geim, S. V. Morosov, I. V. Grigorieva, D. Jiang, Y. Zhang, A. A. Firsov, and S. V. Dubonos, "Electric Field Effect in Atomically Thin Carbon Films," Science (80). **306**(5696), 666–669 (2016).
19. F. Wang, Y. Zhang, C. Tian, C. Girit, A. Zettl, M. Crommie, and Y. R. Shen, "Gate-variable optical transitions in graphene," Science **320**(5873), 206–209 (2008).
20. Z. T. Ma, Z. X. Geng, Z. Y. Fan, J. Liu, and H. D. Chen, "Modulators for Terahertz Communication: The Current State of the Art," Research **2019**(3), 1–22 (2019).
21. Z. Wang, J. Qiao, S. Zhao, S. Wang, C. He, X. Tao, and S. Wang, "Recent progress in terahertz modulation using photonic structures based on two-dimensional materials," InfoMat **3**(10), 1110–1133 (2021).
22. L. Ju, B. Geng, J. Horng, C. Girit, M. Martin, Z. Hao, H. A. Bechtel, X. Liang, A. Zettl, Y. R. Shen, and F. Wang, "Graphene plasmonics for tunable terahertz metamaterials," Nat. Nanotechnol. **6**(10), 630–634 (2011).
23. W. Gao, J. Shu, K. Reichel, D. V. Nickel, X. He, G. Shi, R. Vajtai, P. M. Ajayan, J. Kono, D. M. Mittleman, and Q. Xu, "High-contrast terahertz wave modulation by gated graphene enhanced by extraordinary transmission through ring apertures," Nano Lett. **14**(3), 1242–1248 (2014).
24. M. Kim, S. Kim, and S. Kim, "Ultra-compact integrated terahertz modulator based on a graphene metasurface," Opt. Lett. **46**(3), 605–608 (2021).
25. Z. Li and N. Yu, "Modulation of mid-infrared light using graphene-metal plasmonic antennas," Appl. Phys. Lett. **102**(13), 131108 (2013).
26. W. Zhu, I. D. Rukhlenko, and M. Premaratne, "Graphene metamaterial for optical reflection modulation," Appl. Phys. Lett. **102**(24), 241914 (2013).
27. M. F. Craciun, S. Russo, M. Yamamoto, and S. Tarucha, "Tuneable electronic properties in graphene," Nano Today **6**(1), 42–60 (2011).
28. T. Low and P. Avouris, "Graphene plasmonics for terahertz to mid-infrared applications," ACS Nano **8**(2), 1086–1101 (2014).
29. V. E. Rogalin, I. A. Kaplunov, and G. I. Kropotov, "Optical Materials for the THz Range," Opt. Spectrosc. **125**(6), 1053–1064 (2018).
30. M. Naftaly and R. E. Miles, "Terahertz time-domain spectroscopy of silicate glasses and the relationship to material properties," J. Appl. Phys. **102**(4), 043517 (2007).
31. N. K. Emani, T. F. Chung, X. Ni, A. Kildishev, Y. P. Chen, and A. Boltasseva, "Electrically tunable damping of plasmonic resonances with graphene," Nano Lett. **12**(10), 5202–5206 (2012).
32. G. W. Hanson, "Dyadic Green's functions and guided surface waves for a surface conductivity model of graphene," J. Appl. Phys. **103**(6), 064302 (2008).
33. L. A. Falkovsky, "Optical properties of graphene," J. Phys.: Conf. Ser. **129**, 012004 (2008).
34. M. Liu, X. Yin, E. Ulin-Avila, B. Geng, T. Zentgraf, L. Ju, F. Wang, and X. Zhang, "A graphene-based broadband optical modulator," Nature **474**(7349), 64–67 (2011).
35. M. Liu, X. Yin, and X. Zhang, "Double-layer graphene optical modulator," Nano Lett. **12**(3), 1482–1485 (2012).
36. S. S. Harsha, N. Laman, and D. Grischkowsky, "High-Q terahertz Bragg resonances within a metal parallel plate waveguide," Appl. Phys. Lett. **94**(9), 091118 (2009).